
Synthesizing Unrestricted False Positive Adversarial Objects Using Generative Models

Martin Kotuliak
ETH Zurich
komartin@student.ethz.ch

Sandro E. Schönborn
ABB Future Labs
sandro.schoenborn@ch.abb.com

Andrei Dan
ABB Future Labs
andrei.dan@ch.abb.com

Abstract

Adversarial examples are data points misclassified by neural networks. Originally, adversarial examples were limited to adding small perturbations to a given image. Recent work introduced the generalized concept of unrestricted adversarial examples, without limits on the added perturbations. In this paper, we introduce a new category of attacks that create unrestricted adversarial examples for object detection. Our key idea is to generate *adversarial objects* that are *unrelated* to the classes identified by the target object detector. Different from previous attacks, we use off-the-shelf Generative Adversarial Networks (GAN), without requiring any further training or modification. Our method consists of searching over the latent normal space of the GAN for adversarial objects that are wrongly identified by the target object detector. We evaluate this method on the commonly used Faster R-CNN ResNet-101, Inception v2 and SSD Mobilenet v1 object detectors using logo generative iWGAN-LC and SNGAN trained on CIFAR-10. The empirical results show that the generated adversarial objects are indistinguishable from non-adversarial objects generated by the GANs, transferable between the object detectors and robust in the physical world. This is the first work to study unrestricted false positive adversarial examples for object detection.

1 INTRODUCTION

Deep Neural Networks (DNN) are increasingly used in safety critical applications. One important use case is using machine learning for traffic sign detection. With the

popularity of DNN models used in critical applications, the threat of creating malicious imagery also increases. These attacks are called adversarial examples. The role of an adversarial example is to fool the DNN in classifying the input image differently from how a human would.

Neural networks have been shown to be vulnerable to adversarial examples in [Szegedy et al., 2013]. Follow up work [Carlini and Wagner, 2017, Goodfellow et al., 2015, Moosavi-Dezfooli et al., 2016, Su et al., 2019] improved the algorithms to generate adversarial examples based on small perturbations of the input. [Song et al., 2018, Wang et al., 2019] use generative adversarial networks (GAN) to create unrestricted adversarial examples, instead of perturbing existing images. While many techniques focus on digital attacks, where the attacker has access to either the camera or the IT infrastructure, it is important to explore and understand feasible physical attacks in more detail.

In this work, we introduce a new attack that synthesizes unrestricted adversarial examples for object detection. We believe this is the first work that investigates unrestricted adversarial examples that cause false positives for object detection. Our method generates, using off-the-shelf GANs, adversarial objects that are wrongly identified by object detectors. We evaluate our attack in a physical world setting and observe that the adversarial objects are robust to the positioning of the camera.

Figure 1 shows an overview of the new attack, instantiated for traffic sign detectors and using a GAN that generates logos. Since logos are frequently found on cars, buildings, shops, billboards, a malicious logo that attacks a traffic sign DNN detector has small changes of raising suspicion. Our algorithm optimizes latent variables, such that the GAN synthesizes logos that look natural and are adversarial to the target traffic sign detector. In this example, the logo is detected as a danger sign by the traffic sign DNN detector.

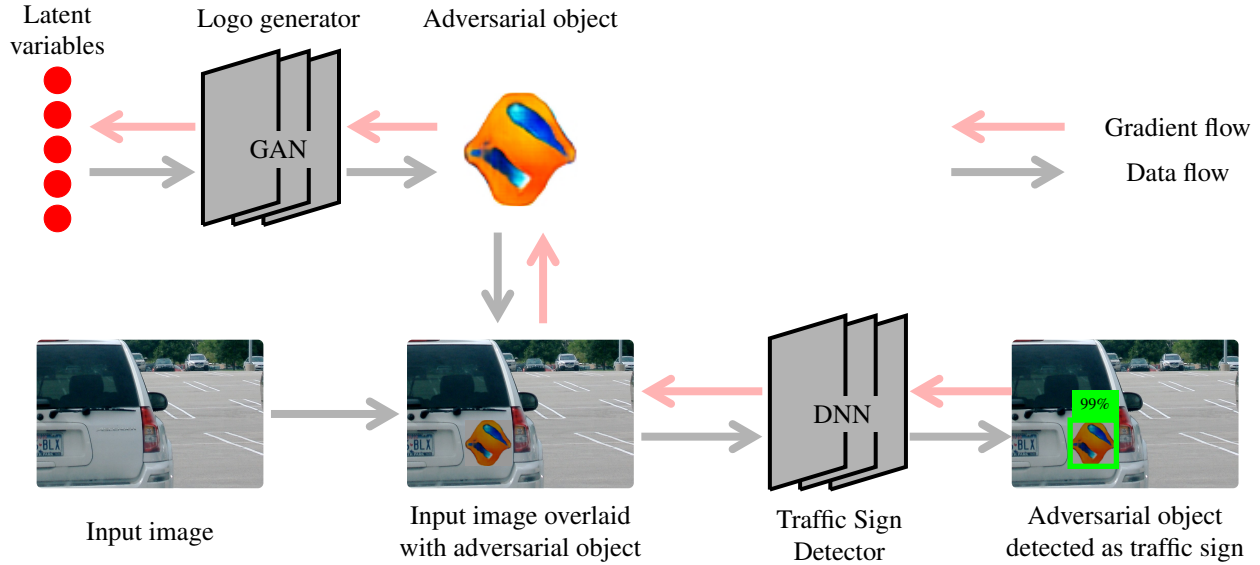


Figure 1: Overview of our method for creating adversarial objects using off-the-shelf GAN.

Our Contributions The main contributions of this work are:

1. We introduce a new attack category, namely unrestricted false positive adversarial objects, that are unrestricted adversarial examples for object detection which resemble other natural objects in physical world.
2. The paper describes a novel and effective algorithm for generating adversarial objects for object detection neural networks, using pre-trained GANs.
3. We implement our algorithm and evaluate it using widely used Faster R-CNN Object Detection networks based on ResNet-101 and Inception v2 and the SSD Mobilenet, trained for traffic sign detection. To generate the adversarial objects, we evaluate two generative models: logo generating iWGAN-LC and the SNGAN trained on CIFAR-10.
4. We demonstrate the transferability of the synthesized adversarial examples between different object detection networks and the robustness of the attacks in a physical setup.

In the next section, we provide background information on adversarial examples. Next, in section 3 we explain the theory behind our attack and we present the results of our empirical evaluation in section 4. Before concluding, we present related work in section 5.

2 BACKGROUND

2.1 ADVERSARIAL EXAMPLES

Let \mathcal{I} be the set of all digital images and $\mathcal{O} \subseteq \mathcal{I}$ a subset of natural images from a specific domain (e.g., handwritten numbers). Oracle $o : \mathcal{I} \rightarrow \{1, 2, \dots, K, \nu, \phi\}$ maps images in its domain \mathcal{O} to K classes, all other natural images to a class ν , and unnatural (noisy) images to class ϕ . The oracle o represents a human observer. The classifier $f : \mathcal{I} \rightarrow \{1, 2, \dots, K\}$ maps all digital images to one of K classes. As defined in [Song et al., 2018], a *perturbation-based adversarial example* x is an image x obtained by perturbing an original image x' such that the classifier f maps the original and the perturbed images to different classes. The perturbation must be small enough to fool the classifier but not the oracle.

Definition 1 (Perturbation-Based Adversarial Examples). *Perturbation-based adversarial examples \mathcal{A}_p are defined for a (test) subset of images $\mathcal{T} \subseteq \mathcal{O}$, and a small perturbation bound ϵ as:*

$$\mathcal{A}_p \triangleq \{x \in \mathcal{O} \mid \exists x' \in \mathcal{T} : \|x - x'\| \leq \epsilon \wedge f(x) \neq f(x') = o(x) = o(x')\}$$

To generate a perturbation-based adversarial example for an object classifier, one must solve an optimisation problem. [Yuan et al., 2019] defines a general optimisation problem:

$$\begin{aligned} \min_{x'} & \|x' - x\| \\ \text{s.t.} & f(x') \neq f(x) \\ & x \in [0, 1] \end{aligned}$$

where $\|\cdot\|$ measures the distance between the adversarial example and the original image. Large perturbations might fool both the human and the classifier, making the attack fail the task, or make the adversarial example be outside of intended domain \mathcal{O} .

The distance function between the original image and the adversarial example measures how close the images are to each other. An ideal distance function would model human perception, rather than the pixel-based distance. [Rozsa et al., 2016] tried to create a more complex function to capture human vision through luminance, contrast, and structural measures. [Jang et al., 2017] based the similarity function on Fourier transformations around the edges. In practice, most research work uses the l_p distance as a proxy.

The optimization of the general problem is hard due to the high non-linearity of the distance functions [Carlini and Wagner, 2017]. For a summary on different approaches to reformulating the problem, we refer the reader to [Yuan et al., 2019].

[Carlini and Wagner, 2017] solved the optimisation problem for perturbations η on top of original image x' :

$$\min_{\eta} \|\eta\|_p + \kappa g(x' + \eta, x') \quad (1)$$

$$\text{s.t. } x' + \eta \in [0, 1]^n \quad (2)$$

in an iterative manner, using gradient descent. The function g evaluates classification error of the target classifier. Value of g for an original and an adversarial image is low if they are classified to different classes, and high if they are classified as the same class. The l_p norm $\|\eta\|_p$ regularizes the amount of perturbation applied. κ is a unitless trade-off parameter for regularization. Finally, the constraint enforces the image with perturbation is still a valid picture with pixel values in the range of $[0, 1]$.

2.2 GENERATIVE ADVERSARIAL NETWORK

A Generative Adversarial Network (GAN) is a network consisting of a discriminator and a generator. The discriminator’s goal is to distinguish generated images from real ones. The generator takes as an input a latent variable $z \sim \mathcal{N}(0, 1)$ and outputs an image. Its goal is to fool the discriminator to not recognize that the image is artificial. This goal is expressed as a loss function during the training phase of the GAN. GANs can be conditioned to generate images in a specific class c : $\text{GAN}(z, c)$.

2.3 UNRESTRICTED ADVERSARIAL EXAMPLES

[Song et al., 2018] explores the idea of creating adversarial images that are not constrained by a distance func-

tion. The restrictions for adversarial images are lifted, and they only require the classification to be different from the oracle label.

Definition 2 (Unrestricted Adversarial Examples). [Song et al., 2018] defines unrestricted adversarial examples as $\mathcal{A}_u \triangleq \{x \in \mathcal{O} \mid f(x) \neq o(x)\}$

They train a GAN network that approximates the domain \mathcal{O} of images. The GAN is further conditioned on the class c of images to generate. Assuming that a perfect GAN network generates natural images of class c if z is sampled from the GAN’s latent distribution Q : $\forall z \sim Q, c : \text{GAN}(z, c) \in \mathcal{O} \wedge o(\text{GAN}(z, c)) = c$, they find latent variables z such that $f(\text{GAN}(z, c)) \neq c$. The optimization problem is then simplified as:

$$\min_z g'(\text{GAN}(z, c), c)$$

for a new classification error function g' . g' evaluates to a low value for a latent variable z and a target class c , if an image $\text{GAN}(z, c)$ is not classified as c . It is evaluated to a greater value if it is classified as c . They overcome issues of using distance functions to measure perturbations by using GAN generated images.

2.4 WHITE-BOX VS BLACK-BOX ATTACK

[Yuan et al., 2019] classifies the attacks in two categories depending on the attacker model. A white-box attacker has full access to the attacked DNN, can view individual trained parameters and perform operations with it. On the other hand, a black-box attack limits the access to the target DNN. The attacker is only allowed to feed images into the target network and observe outputs and cannot directly observe the inner working of the model.

2.5 ADVERSARIAL OBJECTS

When a physical world scenario is considered, the attacker can not perturb the entire scene. Most of the physical world attacks are conducted using adversarial stickers. An adversarial sticker is a printable 2D shape with a filling that is chosen by the attacker [Sharif et al., 2016, Eykholt et al., 2018b, Eykholt et al., 2018a, Chen et al., 2018].

In computer vision, we discriminate the models between classifiers and object detectors. A classifier outputs the class of an image, whereas detectors label objects in the digital image. [Lu et al., 2017] showed that attacking an object detector is more difficult than attacking an object classifier. The object detector finds an object in the image whereas the object classifier only outputs the class of the image. An adversarial object is an adversarial example attacking the object detector.

Successful adversarial examples are either classified as false positives (FP) or false negatives (FN). A false negative attack occurs when a perturbed input is classified differently from the input without perturbation, e.g. ignored or incorrectly classified. A false positive is when an input which would not be classified at all is assigned a class. A FP attack makes object detectors detect at least one object of the target class, even though it is not present.

2.6 OBJECT DETECTORS

Faster R-CNN [Ren et al., 2015] is a neural network architecture for object detection. It first generates generic object bounding box proposals, which it then classifies in the second step. The network is optimized for speed, by using only a single CNN for both stages.

The Single Shot Detector [Liu et al., 2016] uses one propagation through the network to detect all objects and assign them classes. It detects a high number of bounding boxes in different sizes, and then picks one bounding box for each object.

3 DESIGN

We present our novel attack that generates unrestricted false positive adversarial objects for object detection.

3.1 UNRESTRICTED FALSE POSITIVE ADVERSARIAL EXAMPLES

The oracle o not only labels objects in domain \mathcal{O} to K classes, as defined in section 2, it also differentiates between all other natural images ν and noisy, unnatural digital images ϕ . A detector d works similarly to the classifier f , however it has an extra class \perp for all undetected images. These correspond to images that the detector does not identify as being one of the K target classes, but as other natural or noisy images (classes ν and ϕ of the observer).

Definition 3 (Unrestricted False Positive Adversarial Examples). *Unrestricted FP adversarial examples are defined as $\mathcal{A}_{fp} \triangleq \{x \in \mathcal{I} \setminus \mathcal{O} \mid o(x) = \nu \wedge d(x) \in \{1, 2, \dots, K\}\}$.*

\mathcal{A}_{fp} is a set of natural images (such that they can occur in physical world) that a detector identifies as one of the K classes, but to a human observer they look like one of many objects in physical world, not part of one of the K categories. Finally, we define the set $\mathcal{M} = \{x \in \mathcal{I} \setminus \mathcal{O} \mid o(x) = \nu\}$ containing all the natural images outside the K target classes.

3.2 ATTACKER MODEL

The attacker model that we consider assumes that he can only augment the physical world. However, to generate the proposed adversarial object, the attacker requires full access to the object detection network (white-box). Our empirical evaluation in section 4 shows the transferability of adversarial objects between different object detection models trained on the same dataset. This allows the attacker to perform an attack without having access to the exact target object detector (black-box).

3.3 EFFECTIVE GENERATION OF UNRESTRICTED FALSE POSITIVE ADVERSARIAL OBJECTS

To generate an object in \mathcal{M} , we choose an arbitrary unconditional GAN such that $\forall z : \text{GAN}(z) \in \mathcal{M} \wedge \exists z : d(\text{GAN}(z)) = \{1, 2, \dots, K\}$. Such a GAN defines a subset of \mathcal{M} . The attacker can select which domain to use by using different GANs.

We optimize for the latent vector z in a loss function \mathcal{L} which is composed of two terms:

$$\mathcal{L} = \mathcal{L}_0 + \kappa \mathcal{L}_1 \quad (3)$$

\mathcal{L}_0 is a term enforcing an adversarial output, \mathcal{L}_1 is enforcing the natural look of the GAN output and κ is a unitless trade-off parameter for regularization.

To perform a targeted attack for a specific class c within \mathcal{O} we can use the loss term:

$$\mathcal{L}'_0 = -\log \Pr[d(\text{GAN}(z)) = c]$$

\mathcal{L}'_0 is forcing the optimizer to find a latent vector z , such that the GAN generates an image which is classified with the target class label c .

An object detection DNN performs both object proposal generation and detection. It takes as input a digital image x' and creates n object proposals that the object detection DNN should identify. Proposals B_1, B_2, \dots, B_n correspond to cropped images of objects in the original image. $B_k(x')$ is the k^{th} object in x' . Since we do not know which proposal will correspond to our adversarial object, \mathcal{L}'_0 must be reformulated as:

$$\mathcal{L}_0 = -\sum_{i=1}^n \log \Pr[d(B_i(\text{GAN}(z) \oplus x')) = c] \quad (4)$$

To generate a physical adversarial object, we first need to simulate it in a digital image and then print it. The

\oplus operation signifies the overlap of the generated object over a small space of original image.

A positive outcome of the new loss function is that the object detection DNN can detect multiple objects in the same adversarial object, increasing the strength of the attack.

For a GAN to create samples approximately from the training distribution, we need to ensure that z follows its intended distribution $z \sim Q$. This is the distribution which was used during training of the generator. For z outside of Q , the generated images look unnatural. For many available GAN networks, Q is a standard normal distribution $z \sim \mathcal{N}(0, I)$. Although we restrict ourselves to normal distributions in this work, it is important to note that the same procedure analogously applies to more complex distributions of z .

We implement the regularization loss \mathcal{L}_1 based on the difference between the intended and the estimated distribution of z . In order to quantify the difference between two distributions, we use a KL divergence:

$$\mathcal{L}_1 = D_{KL}(P||Q) \quad (5)$$

where P is the estimated distribution of current z and Q is its intended distribution.

Given the intended distribution of $z \sim \mathcal{N}(0, I)$, we initialize z by sampling each element from $\mathcal{N}(0, 1)$. To estimate z at each iteration, we assume that each element is drawn from the same normal distribution. We estimate its mean $\hat{\mu}_P$ and variance $\hat{\sigma}_P^2$ by computing them over all elements of z . For $Q = \mathcal{N}(0, 1)$:

$$D_{KL}(P||Q) = \log \frac{1}{\hat{\sigma}_P} + \frac{\hat{\sigma}_P^2 + \hat{\mu}_P^2}{2} - \frac{1}{2} \quad (6)$$

Figure 1 visualizes our framework and the end-to-end optimization. The generation of an adversarial image starts with the input of the target image. The framework internally initializes a latent object vector z by a random draw from $\mathcal{N}(0, I)$ and overlays the picture generated by the GAN on the input image. The object detector scores each candidate bounding box we need for our loss function. The latent object representation z is then updated using a suitable gradient descent method with the overall end-to-end gradient.

Our proposed framework uses only the generator network of the GAN. We therefore just expect a (differentiable) function $\text{GAN}(z)$ creating images from latent representations z . Such functions can potentially also be learned by other frameworks, e.g. (Variational) Auto Encoder [Kingma and Welling, 2013]. The only reason to

use a GAN in our work is the typically more convincing perceptual quality of generated images.

3.4 EXPECTATION OVER TRANSFORMATION

To improve the robustness of the adversarial objects, we implemented the Expectation over Transformation method [Athalye et al., 2017] using translation, brightness, size and smoothing transforms \mathcal{T} . We optimize the expectation value of Equation 3 under application of such transforms to the generated object before patching them onto the background image. Integrating over transforms increased the success rate of adversarial object generation.

3.5 IMPLEMENTATION

Algorithm 1: Generating Unrestricted False Positive Adversarial Objects

input : Background Image x' , Target Detection Class c , Generative Adversarial Network GAN, Object Detector D , Learning Rate λ

output: vector z

$z \leftarrow \text{random}(\mathcal{N}(0, I));$

$counter \leftarrow 0;$

while $counter < 5$ **do**

$t \leftarrow \text{random}(\mathcal{T});$

$z \leftarrow \text{adamUpdate}(z, \nabla_z \mathcal{L}(z, c, t), \lambda);$

if $D(x' \oplus \text{GAN}(z), c) \geq 0.95$ **then**

$counter ++;$

else

$counter \leftarrow 0;$

end

end

We implement the method in TensorFlow 1.12 [Tensorflow, 2020]. We import two frozen graphs into our framework. One corresponding to the target object detector and the other one corresponding to the GAN network. We have a complete view of these two graphs, and we are able to augment them such that we can skip nodes which loose gradient such as rounding. We optimize using TensorFlow’s Adam implementation. In each iteration we apply a random transform to the generated image before stitching onto the background image. Because detection model is DNN we approximate \mathcal{L}_0 (Equation 4) with second to last layer values, before sigmoid function is applied. Loss function optimization is noisy. Therefore, optimization is terminated with success if the detection confidence for our target class surpasses 0.9 five iterations in a row within at most 2,000 iterations, otherwise the case fails. Algorithm 1 shows the generation process.

Table 1: Performance and execution time of object detectors [Arcos-Garcia et al., 2018] used in evaluation.

Object Detector	mAP	Inference [ms]
ResNet-101	95.08	123
Inception v2	90.62	59
SSD Mobilenet	61.64	15

4 EVALUATION

4.1 SETUP

We illustrate our new attack on traffic sign object detection networks. The correct functionality of these detectors is important for autonomous driving applications. We attack three different pre-trained models: two Faster R-CNNs object detectors (using ResNet-101 and Inception v2 as CNN layer) and SSD Mobilenet v1. These models recognize three categories of traffic signs: prohibitory, mandatory and danger. These networks were evaluated in the study on deep neural networks for traffic signs in [Arcos-Garcia et al., 2018]. We chose these networks to cover various possible use cases: the Faster R-CNN networks have a high mean average precision (mAP), while the SSD Mobilenet has a fast inference time. Table 1 summarizes the object detectors used in our experiments, and their performance, as reported in [Arcos-Garcia et al., 2018]. In the rest of the evaluation section, we use the terms ResNet-101, Inception v2 and SSD Mobilenet to denote these three object detectors.

In our experiments, we use the logo generator iWGAN-LC [Sage et al., 2018] to synthesize the adversarial objects. For this logo GAN, the output is a square logo of size 64×64 pixels. An attacker could add the realistically looking logos in places visible to the camera used for the traffic sign detection (other cars in traffic, billboards). Figure 3 shows sample adversarial logos generated by the logo GAN for each category of traffic signs, together with real traffic signs from each category of the object detectors.

To propagate the gradient through the Faster R-CNN neural networks, we used the algorithm presented in [Chen et al., 2018], which overcomes the non-differentiability of the two-stage process of these networks.

Since SSD Mobilenet is a one phase detector, we adapt the generation process. As a first step, SSD Mobilenet resizes original image of size 1200×720 to 300×300 . The logo is resized $4\times$ on x-axis and $2.4\times$ on y-axis.

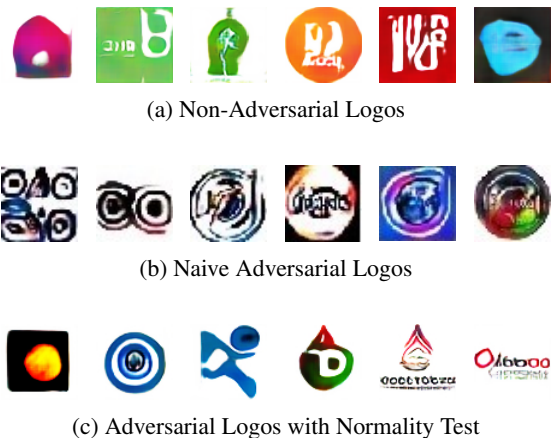


Figure 2: Comparison between non-adversarial, naive adversarial, and adversarial logos generated by adding the normality test to the loss function.

The resizing operation is differentiable, therefore the gradient can be propagated through. Downsizing means that the gradient is distributed among multiple pixels of the original logo. The generation process stagnates and does not produce adversarial objects. To address this challenge, we exploit the detection process of SSD Mobilenet, which detects bounding boxes of various scales. We resize the background image to 300×300 and overlap the object over the resized image. While the adversarial object is optimized on large bounding boxes of SSD, it is also effective on small bounding boxes.

4.2 NORMALITY TEST IN LOSS FUNCTION

To illustrate the importance of the normality test in the loss function, we generate three types of logos. First, we generate benign logos by randomly sampling a latent vector from normal distribution $\mathcal{N}(0, I)$. Second, we generate adversarial image by minimizing detection loss only thereby ignoring the distribution loss by setting $\kappa = 0$ in (Equation 3) (naive adversarial logos). The quality of naive adversarial logos is visibly lower. The propagated gradient can change the input latent vector such that the likelihood of a vector being sampled from normal distribution is low. The probability that these latent variables are encountered during training process of the GAN is negligible. Therefore, the generator outputs a logo which looks artificial. The third group of logos are adversarial logos that were generated by using the normality test in the loss function (Equation 5).

Figure 2 shows all the three types of logos. We observe that the logos with a high variance look unnatural, whereas the non-adversarial and adversarial logos have a better quality. Importantly, we observe that the adver-



Figure 3: Adversarial objects for three classes of traffic signs attacking three different object detection networks

adversarial logos have a similar natural look compared to the non-adversarial logos.

4.3 IMPROVING ADVERSARIAL ROBUSTNESS

To improve the robustness of the adversarial objects, we add random transformations to the input during the generation process, described in [Athalye et al., 2017]. Additionally, these transformations speed up the generation process, due to a broader exploration of the latent space. We implement four types of transformations: 1) Translation: the adversarial object is shifted to different position onto the input image; 2) Brightness: the overall brightness of image with adversarial object is changed; 3) Size: the adversarial object is resized; 4) Smoothing: a smoothing Bayesian filter is applied to the image with adversarial object.

At each iteration, we add small random perturbations to these parameters. We build three experiments, to simulate various physical world conditions. We see that the robustness of the adversarial logos with transformation is better, but the difference is small. However, the success rate of generating an adversarial logo in 2000 iterations increased by 10%. Our hypothesis is that the logo GAN creates a robust image with large areas of the same color. Moreover, these areas are clearly separated. The robustness gains are small, but the success rate of generating adversarial logos is improved by the transformations.

When using the transformations, individual success rates of ResNet-101, Inception v2, and SSD Mobilenet are 67%, 76% and 5% respectively. Even though the success rate for SSD Mobilenet is low, attacker is not constrained by time to perform the attack.

Table 2: Transferability of adversarial objects between different object detectors. The rows correspond to the originally attacked model. The columns show transferability to the target models.

	Resnet-101	Inception v2	SSD
Resnet-101	–	64.36%	16.83%
Inception v2	50.88%	–	28.07%
SSD	21.43%	39.29%	–

4.4 TRANSFERABLE ADVERSARIAL OBJECTS

Given the three object detectors, we evaluate the transferability of the adversarial objects. Even if an attacker does not have access to the object detector architecture, it is possible to perform black-box attacks by training different DNN and generating adversarial object on it.

Table 2 shows our transferability experiment results. The two Faster R-CNNs have a high transferability, whereas the attacks are less transferable to the SSD Mobilenet. Given that the Faster R-CNNs share a significant portion of the DNN architecture, these results are expected. Overall, Table 2 shows that the adversarial objects generated with our algorithm are transferable between object detectors, even if they are based on completely different architectures.

4.5 PHYSICAL WORLD EXPERIMENT

For the physical test, we generate 9 adversarial logos for all pairs of attacked classes (prohibitory, mandatory, dan-



Figure 4: Photo taken from position 4 with adversarial objects identified as traffic signs by the object detectors.

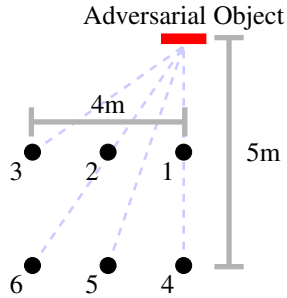


Figure 5: Bird's-eye view of the six positions of the camera for the physical world experiment.

ger) and detection networks (Faster R-CNN ResNet-101, Faster R-CNN Inception v2, SSD Mobilnet v1). After the generation, the logos are printed using a standard office printer on a regular paper, resized to $20 \text{ cm} \times 20 \text{ cm}$.

For each logo, we take six photos from different distances and angles. Figure 5 shows the six positions we have used. Photos are taken using a iPhone X camera with telephoto $f/2.4$ aperture. Figure 4 shows an example photo taken from position 4.

Finally, the photos are down-sampled to 1200×720 pixels, and fed into the three detection networks. Table 3 shows the confidence of each network in detecting given class for each adversarial logo. Positions 3 and 6 give the lowest confidence values on average, due to the angle and distance from the logo. We observe the transferability of adversarial objects in physical world between the two Faster R-CNNs as well. SSD Mobilnet under-performs due to its low detection performance. Additionally, we test two non-adversarial logos in the physical world and they are not detected from any of the six positions.

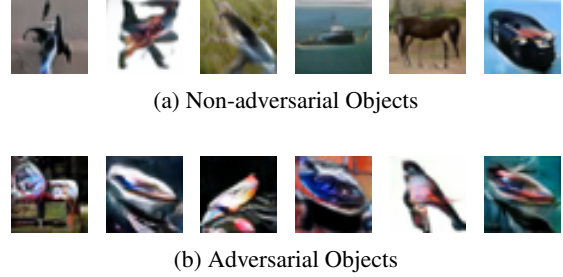


Figure 6: Comparison between non-adversarial and adversarial objects generated by the SNGAN trained on the CIFAR-10 dataset.

4.6 CIFAR-10 SNGAN





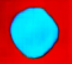




To further evaluate our attack, we train a SNGAN [Miyato et al., 2018] using the CIFAR-10 dataset. We have used the implementation described in [Yang, 2018]. Figure 6 shows samples of adversarial objects generated by this GAN, compared to non-adversarial objects. We observe that the non-adversarial examples have a similar quality with the adversarial objects. This strengthens our confidence that our attack method generates adversarial objects that look as natural as the normal images synthesized by the generative model.

5 RELATED WORK

[Song et al., 2018] employs GAN networks to create examples which a human observer classifies differently than a classifier. The main difference from our work is the attack setting. In their work, the GAN creates images from the same domain as the target classifier. We can use off-the-shelf pre-trained GANs that synthesize images from domains unrelated to the detected classes of the object detectors (e.g., if the object detector identifies animals, our approach can use a GAN that creates cars as adversarial objects). Our attack can be easier to perform in the physical world and more covert.

[Wang et al., 2019, Xiao et al., 2018] use GANs to directly create adversarial examples without an iterative method. [Wang et al., 2019] creates unrestricted examples, whereas [Xiao et al., 2018] uses GANs to create perturbation-based adversarial examples. [Zhao et al., 2017] uses a GAN and an inverter to find the latent variables. Their attack works by finding a good region of the latent space which creates adversarial examples through a random search algorithm, unlike our approach based on gradient descent. Their work focuses on black-box attacks. [Wang et al., 2019, Xiao et al., 2018, Zhao et al., 2017] need a specially-constructed GAN, whereas our method can work with pre-trained GANs.

Table 3: Detection confidence of object detection DNNs in physical world experiment for 9 adversarial objects.

ResNet-101 Inception v2 SSD									
Category	Prohibitory			Mandatory			Danger		
Target DNN	ResNet	Inception	SSD	ResNet	Inception	SSD	ResNet	Inception	SSD
Pos. 1	99%	98%	–	99%	99%	–	99%	–	–
	98%	99%	54%	99%	99%	–	98%	94%	–
	–	99%	32%	–	–	96%	–	–	–
Pos. 2	99%	98%	60%	99%	99%	–	99%	99%	–
	99%	99%	39%	99%	99%	76%	99%	99%	41%
	–	67%	–	–	–	–	–	43%	44%
Pos. 3	91%	95%	–	99%	–	–	–	99%	–
	92%	98%	36%	76%	99%	93%	20%	99%	–
	–	–	–	–	–	–	–	10%	24%
Pos. 4	99%	99%	91%	99%	99%	99%	99%	99%	–
	99%	99%	35%	99%	99%	97%	80%	99%	95%
	–	99%	97%	–	–	89%	–	69%	–
Pos. 5	97%	99%	54%	99%	99%	99%	99%	99%	–
	99%	99%	45%	99%	99%	98%	89%	99%	57%
	–	91%	–	–	–	99%	–	79%	99%
Pos. 6	84%	99%	89%	99%	31%	99%	–	99%	–
	99%	99%	96%	–	90%	99%	11%	99%	–
	–	–	–	–	–	–	–	–	–

All of the previously mentioned papers explore attacks against classifiers. In our work we explore attacks against object detectors. Additionally, none of them explores attacks in physical world. We believe that real-world perturbations represent a high, as these attacks do not require the access to the camera.

In recent work, [Kurakin et al., 2016, Sharif et al., 2016, Eykholt et al., 2018b, Eykholt et al., 2018a, Chen et al., 2018] explored adversarial examples in physical world. They work by creating adversarial stickers/patches which are put onto other objects, e.g., stop signs. After the camera takes a picture, the augmented stop sign is misclassified/undetected. Moreover, [Eykholt et al., 2018a] looked at creating false positive attacks using current techniques for creating perturbation-based adversarial examples. The detection model recognized the adversarial object as a stop sign, even thought to a human observer it does not look like one. The potential limitation of these approaches is the high salience of such objects. We believe that if the attacker launches a physical attack, it is easy to identify the malicious object and indict the attacker. In our work, the GAN network produces robust adversarial objects which are assimilated in the real world scenery.

The detectors used in [Eykholt et al., 2018a, Chen et al., 2018, Sitawarin et al., 2018] are not ac-

cessible. The missing performance statistics make it hard to judge the attack’s strength. In our work, the detectors are chosen from a published work in traffic sign detection [Arcos-Garcia et al., 2018].

6 CONCLUSION

We defined a new attack for object detectors, based on unrestricted adversarial examples. To synthesize adversarial objects, we use off-the-shelf pre-trained GANs that generate images unrelated to the detected classes of the target neural network. Importantly, the synthesized adversarial objects are indistinguishable from non-adversarial outputs of the GANs, from a human’s perspective. We experimented with the Faster R-CNN ResNet-101, Inception v2 and SSD Mobilenet object detectors trained for traffic sign recognition and used two pre-trained generative models, SNGAN trained on CIFAR-10 and logo generating iWGAN-LC. The evaluation results show that the adversarial objects are transferable between target neural networks (between 16% and 64%). Moreover, we validated the adversarial objects in a physical world setup, which demonstrated their robustness to camera angle and distance to the camera. By introducing unrestricted false positive adversarial objects, we extend the space of attacks and open new directions to investigate the reliability of object detectors.

REFERENCES

- [Arcos-Garcia et al., 2018] Arcos-Garcia, A., Alvarez-Garcia, J. A., and Soria-Morillo, L. M. (2018). Evaluation of deep neural networks for traffic sign detection systems. *Neuro-computing*, 316:332–344.
- [Athalye et al., 2017] Athalye, A., Engstrom, L., Ilyas, A., and Kwok, K. (2017). Synthesizing robust adversarial examples. *arXiv preprint arXiv:1707.07397*.
- [Carlini and Wagner, 2017] Carlini, N. and Wagner, D. (2017). Towards evaluating the robustness of neural networks. In *2017 IEEE Symposium on Security and Privacy (SP)*, pages 39–57. IEEE.
- [Chen et al., 2018] Chen, S.-T., Cornelius, C., Martin, J., and Chau, D. H. P. (2018). Shapeshifter: Robust physical adversarial attack on faster r-cnn object detector. In *Joint European Conference on Machine Learning and Knowledge Discovery in Databases*, pages 52–68. Springer.
- [Eykholt et al., 2018a] Eykholt, K., Evtimov, I., Fernandes, E., Li, B., Rahmati, A., Tramer, F., Prakash, A., Kohno, T., and Song, D. (2018a). Physical adversarial examples for object detectors. *arXiv preprint arXiv:1807.07769*.
- [Eykholt et al., 2018b] Eykholt, K., Evtimov, I., Fernandes, E., Li, B., Rahmati, A., Xiao, C., Prakash, A., Kohno, T., and Song, D. (2018b). Robust physical-world attacks on deep learning visual classification. In *Proceedings of the IEEE Conference on Computer Vision and Pattern Recognition*, pages 1625–1634.
- [Goodfellow et al., 2015] Goodfellow, I., Shlens, J., and Szegedy, C. (2015). Explaining and harnessing adversarial examples. In *International Conference on Learning Representations*.
- [Jang et al., 2017] Jang, U., Wu, X., and Jha, S. (2017). Objective metrics and gradient descent algorithms for adversarial examples in machine learning. In *Proceedings of the 33rd Annual Computer Security Applications Conference*, pages 262–277.
- [Kingma and Welling, 2013] Kingma, D. P. and Welling, M. (2013). Auto-encoding variational bayes. *arXiv preprint arXiv:1312.6114*.
- [Kurakin et al., 2016] Kurakin, A., Goodfellow, I., and Bengio, S. (2016). Adversarial examples in the physical world. *arXiv preprint arXiv:1607.02533*.
- [Liu et al., 2016] Liu, W., Anguelov, D., Erhan, D., Szegedy, C., Reed, S., Fu, C.-Y., and Berg, A. C. (2016). Ssd: Single shot multibox detector. In *European conference on computer vision*, pages 21–37. Springer.
- [Lu et al., 2017] Lu, J., Sibai, H., Fabry, E., and Forsyth, D. (2017). Standard detectors aren’t (currently) fooled by physical adversarial stop signs. *arXiv preprint arXiv:1710.03337*.
- [Miyato et al., 2018] Miyato, T., Kataoka, T., Koyama, M., and Yoshida, Y. (2018). Spectral normalization for generative adversarial networks. *arXiv preprint arXiv:1802.05957*.
- [Moosavi-Dezfooli et al., 2016] Moosavi-Dezfooli, S.-M., Fawzi, A., and Frossard, P. (2016). Deepfool: a simple and accurate method to fool deep neural networks. In *Proceedings of the IEEE conference on computer vision and pattern recognition*, pages 2574–2582.
- [Ren et al., 2015] Ren, S., He, K., Girshick, R., and Sun, J. (2015). Faster r-cnn: Towards real-time object detection with region proposal networks. In *Advances in neural information processing systems*, pages 91–99.
- [Rozsa et al., 2016] Rozsa, A., Rudd, E. M., and Boulton, T. E. (2016). Adversarial diversity and hard positive generation. In *Proceedings of the IEEE Conference on Computer Vision and Pattern Recognition Workshops*, pages 25–32.
- [Sage et al., 2018] Sage, A., Agustsson, E., Timofte, R., and Van Gool, L. (2018). Logo synthesis and manipulation with clustered generative adversarial networks. In *Proceedings of the IEEE Conference on Computer Vision and Pattern Recognition*, pages 5879–5888.
- [Sharif et al., 2016] Sharif, M., Bhagavatula, S., Bauer, L., and Reiter, M. K. (2016). Accessorize to a crime: Real and stealthy attacks on state-of-the-art face recognition. In *Proceedings of the 2016 ACM SIGSAC conference on computer and communications security*, pages 1528–1540.
- [Sitawarin et al., 2018] Sitawarin, C., Bhagoji, A. N., Mosenia, A., Chiang, M., and Mittal, P. (2018). Darts: Deceiving autonomous cars with toxic signs. *arXiv preprint arXiv:1802.06430*.
- [Song et al., 2018] Song, Y., Shu, R., Kushman, N., and Ermon, S. (2018). Constructing unrestricted adversarial examples with generative models. In *Advances in Neural Information Processing Systems*, pages 8312–8323.
- [Su et al., 2019] Su, J., Vargas, D. V., and Sakurai, K. (2019). One pixel attack for fooling deep neural networks. *IEEE Transactions on Evolutionary Computation*, 23(5):828–841.
- [Szegedy et al., 2013] Szegedy, C., Zaremba, W., Sutskever, I., Bruna, J., Erhan, D., Goodfellow, I., and Fergus, R. (2013). Intriguing properties of neural networks. *arXiv preprint arXiv:1312.6199*.
- [Tensorflow, 2020] Tensorflow (2020). tensorflow/docs.
- [Wang et al., 2019] Wang, X., He, K., Song, C., Wang, L., and Hopcroft, J. E. (2019). At-gan: An adversarial generator model for non-constrained adversarial examples. *arXiv preprint arXiv:1904.07793*.
- [Xiao et al., 2018] Xiao, C., Li, B., Zhu, J.-Y., He, W., Liu, M., and Song, D. (2018). Generating adversarial examples with adversarial networks. *arXiv preprint arXiv:1801.02610*.
- [Yang, 2018] Yang, W. (2018). Gan_lib_tensorflow.
- [Yuan et al., 2019] Yuan, X., He, P., Zhu, Q., and Li, X. (2019). Adversarial examples: Attacks and defenses for deep learning. *IEEE transactions on neural networks and learning systems*, 30(9):2805–2824.
- [Zhao et al., 2017] Zhao, Z., Dua, D., and Singh, S. (2017). Generating natural adversarial examples. *arXiv preprint arXiv:1710.11342*.